

Electronic and Optical Properties of 4*H*-Cyclopenta[2,1-*b*:3,4-*b'*]bithiophene Derivatives and Their 4-Heteroatom-Substituted Analogues: A Joint Theoretical and Experimental Comparison[†]

Stephen Barlow,* Susan A. Odom, Kelly Lancaster, Yulia A. Getmanenko, Richard Mason, Veaceslav Coropceanu, Jean-Luc Brédas, and Seth R. Marder

School of Chemistry and Biochemistry and Center for Organic Photonics and Electronics, Georgia Institute of Technology, Atlanta, Georgia 30332-0400

Received: January 26, 2010; Revised Manuscript Received: April 1, 2010

The electronic and optical properties of 2,6-dialkyl and 2,6-bis(5-alkyl-2-thienyl) derivatives of the fused-ring systems 4*H*-cyclopenta[2,1-*b*:3,4-*b'*]bithiophene, 4,4-di-*n*-hexyl-4*H*-cyclopenta[2,1-*b*:3,4-*b'*]bithiophene, 4*H*-cyclopenta[2,1-*b*:3,4-*b'*]bithiophene-4-one, 4-alkyl and 4-aryldithieno[3,2-*b*:2',3'-*d*]pyrrole, 4-phenyldithieno[3,2-*b*:2',3'-*d*]phosphole, 4-phenyldithieno[3,2-*b*:2',3'-*d*]phosphole 4-oxide, dithieno[3,2-*b*:2',3'-*d*]thiophene, dithieno[3,2-*b*:2',3'-*d*]thiophene 4-oxide, and dithieno[3,2-*b*:2',3'-*d*]thiophene 4,4-dioxide have been compared to those of the analogous unbridged 5,5'-substituted 2,2'-bithiophene derivatives using electrochemistry, UV–visible absorption and emission spectroscopy, and DFT and TD-DFT calculations. The planarization in the fused-ring compounds means that the methylene-bridged cyclopentabithiophenes are more readily oxidized than their unbridged bithiophene analogues. In each case, the bridging group (X) lies on a nodal plane of the HOMO; accordingly, within each series of fused-ring compounds, electrochemical oxidation potentials and calculated ionization potentials depend primarily on the inductive donor/acceptor strength of the bridging group. On the other hand, significant LUMO coefficients can be found on X groups with π -donor or acceptor properties; accordingly, the electrochemical reduction potentials, calculated electron affinities, and the energies of the HOMO→LUMO optical transitions depend on both inductive and mesomeric donor and acceptor strengths. In particular, within the 2,6-bis(5-alkyl-2-thienyl) series, increasingly electron-withdrawing bridging groups lead to a bathochromic shift and weakening of the low-energy absorption band relative to that of methylene- or π -donor-bridged examples and also to a loss of vibronic structure, with the compound that has the strongest π -accepting bridge of those examined (X = CO) showing a particularly low-energy and weak band. The fluorescence of acceptor-bridged compounds exhibits greater Stokes shifts and a loss of vibronic structure relative to those of methylene- or π -donor-bridged analogues, with the carbonyl-bridged derivative showing no observable fluorescence. These results can be related to increasing localization of the LUMO on the core and toward the bridging group, leading to increased charge-transfer character for the first excited state. The radical cations of some examples have been generated by chemical oxidation and investigated using visible-NIR and ESR spectroscopy and DFT and TD-DFT calculations. The absorption spectra of the radical cations of the 2,6-bis(5-alkyl-2-thienyl) compounds are generally similar to those previously reported for quaterthiophene derivatives, while the hyperfine couplings obtained from ESR spectra are consistent with delocalization of the unpaired electron over both the core and terminal thienyl rings of the π system.

Introduction

Oligo- and polythiophenes are widely used in materials chemistry, especially as hole-transport materials for field-effect transistors (FETs) and as hole-transport and/or light-harvesting materials in solar cells.^{1–4} Recently, a variety of thiophene-based fused-ring building blocks have been incorporated into materials of this type, including many 3,3'-bridged-2,2'-bithiophene three-ring systems of the type shown in Figure 1: i.e., 4*H*-cyclopenta[2,1-*b*:3,4-*b'*]bithiophene (X = CH₂)^{5–8} and related systems in which the bridging carbon atom in the 4-position is substituted (e.g., X = CR₂, CF₂, C(OCH₂CH₂O))^{9–13} or sp² hybridized (e.g., X = CO, C=C(CN)₂, C=CRR', C=C(CN)(S(O)₂R))^{10,11,14–19} or in which it is replaced with a heteroatom-based group to afford a dithieno[3,2-*b*:2',3'-*d*]borole,²⁰ dithieno[3,2-*b*:2',3'-*d*]silole (X = SiR₂, SiAr₂),^{21–23}

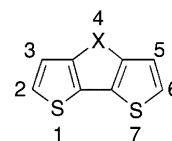
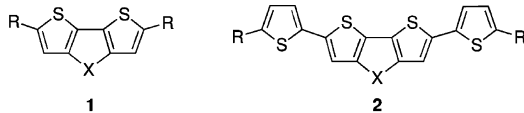


Figure 1. Generalized structure and position labeling for 4*H*-cyclopenta[2,1-*b*:3,4-*b'*]bithiophene derivatives.

dithieno[3,2-*b*:2',3'-*d*]pyrrole (X = NR, NAr),^{24–35} dithieno[3,2-*b*:2',3'-*d*]phosphole (X = PR, PAr),^{36–39} or one of the corresponding metal complexes (e.g., X = P(AuCl)Ph, P(W(CO)₅)Ph),⁴⁰ dithieno[3,2-*b*:2',3'-*d*]phosphole 4-oxide (X = P(O)R, P(O)Ar),^{36–39,41} dithieno[3,2-*b*:2',3'-*d*]phosphole 4-sulfide (X = P(S)Ar),³⁷ dithieno[3,2-*b*:2',3'-*d*]thiophene (X = S),^{33,34,42–60} dithieno[3,2-*b*:2',3'-*d*]thiophene 4-oxide (X = SO),^{60,61} or dithieno[3,2-*b*:2',3'-*d*]thiophene 4,4-dioxide (X = SO₂).^{47,60–64} The introduction of these fused-ring systems has often been used to modify the electronic and/or optical properties of the

[†] Part of the “Michael R. Wasielewski Festschrift”.

* Corresponding author. E-mail: stephen.barlow@chemistry.gatech.edu.

CHART 1: Structures of Compounds Investigated^a


	X	R				R'			
		1	1'	2	2'	1	1'	2	2'
a	no bridge	<i>n</i> -C ₆ H ₁₃	Me	<i>n</i> -C ₇ H ₁₅	Me				
b	CH ₂	—	Me	<i>n</i> -C ₉ H ₁₉	Me				
c	C(<i>n</i> -C ₆ H ₁₃) ₂	—	—	<i>n</i> -C ₉ H ₁₉	—				
d	CO	—	Me	<i>n</i> -C ₉ H ₁₉	Me				
e	NR'	ⁿ Bu	Me	—	—	^t Bu	Me	—	Me
f	N(C ₆ H ₄ -4-R')	ⁿ Bu	Me	—	Me	^t Bu	Me	—	Me
g	N[C ₆ H ₂ -3,4,5-(R'O) ₃]	—	Me	<i>n</i> -C ₇ H ₁₅	Me	—	Me	<i>n</i> -C ₁₂ H ₂₅	Me
h	PPh	—	Me	—	Me				
i	P(O)Ph	—	Me	<i>n</i> -C ₁₀ H ₂₁	Me				
j	S	ⁿ Bu	Me	<i>n</i> -C ₇ H ₁₅	Me				
k	SO	—	Me	<i>n</i> -C ₁₀ H ₂₁	Me				
l	SO ₂	—	Me	<i>n</i> -C ₁₁ H ₂₃	Me				

^a Primed compound numbers denote compounds studied computationally, while unprimed compound numbers denote experimentally investigated compounds.

materials; however, the bridge can also provide a point of attachment for groups to increase solubility or to impart chirality,^{27,30} while the introduction of planar units may favor intermolecular π -stacking.^{58,65} In view of the frequent incorporation of building blocks of this type into more complex conjugated architectures, a detailed understanding of the effects of the group in the 4-position on the electronic properties of the ring system would be valuable. However, although data for 4*H*-cyclopenta[2,1-*b*:3,4-*b'*]bithiophenes and their heteroatom-bridged analogues have been reviewed,^{66,67} only a few experimental studies have made direct comparisons between different members of this series.^{10,11,24,36–39,60} Here we present a joint theoretical and experimental comparison of the electronic and optical properties of 4*H*-cyclopenta[2,1-*b*:3,4-*b'*]bithiophene derivatives incorporating a wide range of carbon- and heteroatom-based groups in the 4-position, specifically focusing on the 2,6-dialkyl-4*H*-cyclopenta[2,1-*b*:3,4-*b'*]bithiophene (**1**) and 2,6-bis-(5-alkyl-2-thienyl)-4*H*-cyclopenta[2,1-*b*:3,4-*b'*]bithiophene species (**2**), shown in Chart 1. Compounds of type **1** allow comparison of the properties of the fused-ring cores in relative isolation; the 2,6-dialkyl groups serve to stabilize the corresponding radical cations and only slightly perturb the optical properties of the neutral species relative to those of the unsubstituted core. Compounds of type **2** serve as models for the incorporation of these cores into more extended π systems. Moreover, quaterthiophenes and their fused analogues of type **2** have been used in organic electronics, primarily in p-channel FETs,^{11,52,55,60,68–71} but also when bearing strongly electron-withdrawing R and/or X groups, in n-channel devices,^{11,12,18,21,22,71} and, in some cases, as lumophores in light-emitting diodes.⁶² The analogous nonfused bithiophene and quaterthiophene derivatives (**1a** and **2a**) are also included in the study for comparison.

Results and Discussion

Compounds Investigated. The 4*H*-cyclopenta[2,1-*b*:3,4-*b'*]bithiophene derivatives under consideration here are summarized in Chart 1. Compounds of type **2** containing a wide

range of bridging groups, X, were studied experimentally, while a more limited set of compounds of type **1** were examined experimentally; DFT and TD-DFT calculations (B3LYP functional, 6-31G(d,p), and for calculating electron affinities (EAs), 6-31+G(d) basis sets) were performed for a wide range of compounds of both classes. The terminal alkyl groups (modeled as methyl groups in the calculations) were incorporated into the structures to increase the solubility of the compounds and also to increase the stability of the corresponding radical cations;⁷² unsubstituted analogues of compounds of both types **1** and **2** typically exhibit irreversible electrochemistry due to polymerization of the radical ions.^{6,9,10,24,25} The synthesis and characterization of the experimentally studied compounds are described in the Supporting Information, along with details of the computational methodology.

Frontier Molecular Orbitals. The HOMOs and LUMOs obtained from DFT calculations are shown for selected compounds in Figure 2. Those for the remaining compounds are given in the Supporting Information (Figures S1 and S2). The HOMO-1s are also shown, due to their role in the absorption spectra of some of the radical cations (vide infra). The HOMOs for all the fused-ring compounds of type **1'** are qualitatively similar to one another and to those of the nonfused bithiophene model **1a'** (as well as to those shown in previous studies of compounds of this type^{24,56,73–75}). This orbital can be regarded as an out-of-phase combination of two local thiophene HOMOs. Significantly, the HOMOs have negligible coefficients on the X groups, with only very small contributions from the oxygen p-orbitals of X = P(O)Ph, SO, and SO₂ derivatives (**1i'**, **1k'**, and **1l'**, respectively), suggesting that the major influence of X upon the HOMO energy should be inductive. The LUMOs are also similar to those of bithiophene, but the X atom makes significant contributions. In particular, X = NR, NAr, and S derivatives (**1e'**–**1g'**, **1j'**) act as π -donors, with N or S p π -orbitals making destabilizing (out-of-phase) contributions to the LUMO. On the other hand, the X = CO derivative (**1d'**) acts as a strong π -acceptor, with the LUMO being an in-phase combination of the local LUMOs of bithiophene with a C=O

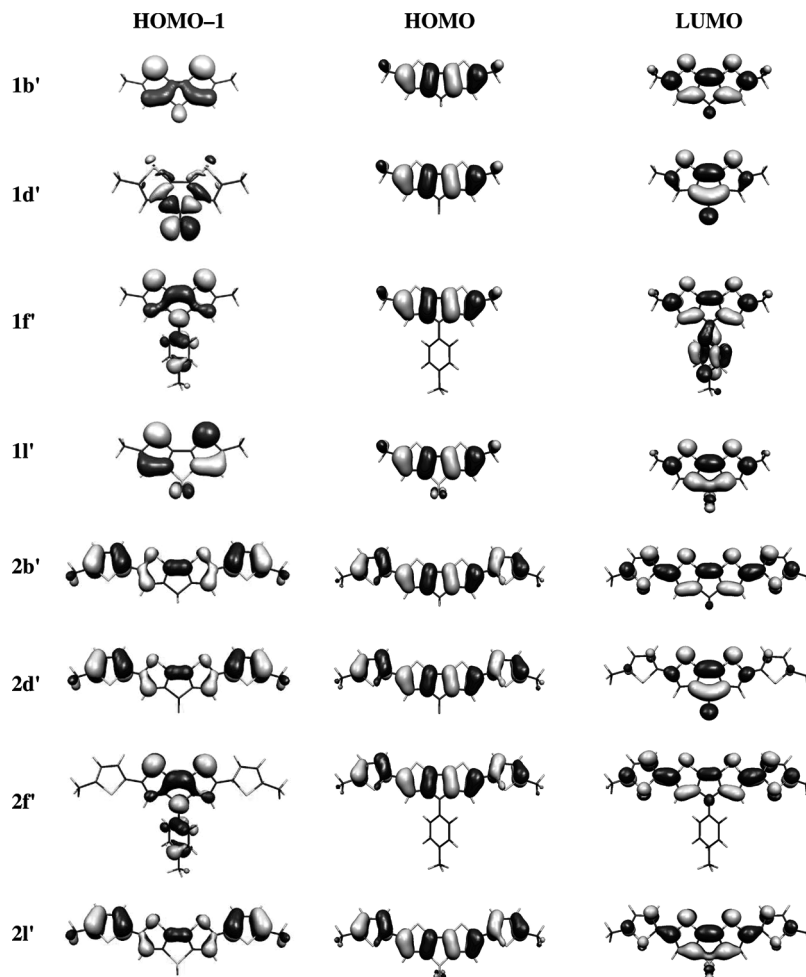


Figure 2. Molecular orbitals for selected cyclopentabithiophene and dithienyl cyclopentabithiophene derivatives according to B3LYP/6-31G(d,p) calculations.

π^* -orbital. Stabilizing π -acceptor interactions are also found in the LUMOs of **1h'**, **1i'**, **1k'**, and **1l'**, where the relevant contribution from X is a local P–Ph, P–O, or S–O σ^* -orbital. Thus, the choice of X substituent is anticipated to influence the LUMO energy through both inductive and mesomeric effects. The HOMO-1s are considerably more variable in composition. Some show clear similarities to that of bithiophene; others are π -orbitals of different symmetry; and that of the X = CO derivative (**1d'**) is best described as a combination of an oxygen 2p lone pair lying in the molecular plane with σ -bonding orbitals of the fused-ring framework.

The HOMOs for compounds of type **2** are all qualitatively similar to one another and to that of the nonfused compound, **2a'** (and to those of the previously published orbitals for compounds of this class^{26,38}). They can be regarded as resulting from the highest-energy combination of the local HOMOs of the fused-ring core and the thienyl substituents, and as with compounds of type **1'**, there is no appreciable HOMO density on the X groups. The LUMOs of all the compounds of type **2'** can be regarded as in-phase combinations of the local LUMO of the appropriate fused-ring core (**1'**) and empty thienyl-based orbitals; i.e., π donor X groups make out-of-phase contributions to the LUMO (as previously seen for an analogue of **2e'** with R = H²⁶), and π -acceptors make in-phase contributions. Interestingly, the LUMO in **2d'** has substantially larger coefficients on the fused-ring core, with only slight extension onto the terminal thienyl groups; this can be related to the X = CO compound being that with the lowest-energy LUMO, which

arises from the significant C=O π^* contribution to the local LUMO of the fused-ring core. The HOMO-1s for compounds of type **2** behave in a more regular fashion than those of type **1**. All are π -orbitals that are clearly related to, and have the same effective symmetry as, that of **2a'**. However, there are varying contributions from the bridging groups—in particular from the heteroatoms of the X = NR, NAr, and S examples (**2e'–g'**, **2j'**) and the aryl groups of the NAr derivatives (**2f'**, **2g'**)—and contributions from the terminal thienyl groups are considerably reduced in the dithienopyrroles (**2e'–g'**).

Electrochemistry, Ionization Potential, and Electron Affinity. To compare the ability of the different dialkyl-4*H*-cyclopenta[2,1-*b*:3,4-*b'*]bithiophene cores to act as donors in the electron-transfer sense, cyclic voltammograms were acquired in 0.1 M dichloromethane solutions of tetra-*n*-butylammonium hexafluorophosphate. The cyclic voltammograms are shown in the Supporting Information (Figures S3–5), along with values of $E_{\text{ox}} - E_{\text{red}}$ (Table S4), while the estimated half-wave potentials are summarized in Table 1. The 2,6-dialkyl-substituted *N*-alkyl- and *N*-aryldithieno[3,2-*b*:2',3'-*d*]pyrroles, **1e** and **1f**, respectively, both exhibit a reversible one-electron oxidation, in contrast to analogous compounds without the 2,6-alkyl substituents.^{24,76} The 5,5'-dialkyl-2,2'-bithiophene and 2,6-dialkyldithieno[3,2-*b*:2',3'-*d*]thiophene, **1a** and **1j**, show EC-type oxidations (i.e., $I_{\text{red}} < I_{\text{ox}}$) which are, nonetheless, considerably more reversible than those of the analogous compounds without 2,6-substituents.²⁴ Comparison of the half-wave potentials indicates that the order of electron-transfer-donor strength decreases in the order NR-

TABLE 1: Electrochemical Half-Wave Potentials (V) vs $\text{FeCp}_2^{+/0}$ in Dichloromethane/0.1 M $n\text{Bu}_4\text{NPF}_6$ and DFT Gas-Phase Adiabatic Ionization Potentials and Electron Affinities (eV) for Cyclopentabithiophene and Dithienyl Cyclopentabithiophene Derivatives

compound	$E_{1/2}^{2+/+}$	$E_{1/2}^{+/0}$	$E_{1/2}^{0/-}$	IP	EA ^a
1a	-	+0.69 ^b	-	6.68	-0.06
1e	-	+0.23	-	6.27	0.49
1f	-	+0.38	-	6.21	0.20
1j	-	+0.66 ^{b,c}	-	5.97	0.16
2a	+0.71	+0.47 ^d	-	5.93	-1.05
2b	+0.59	+0.17 ^d	-	5.73	-0.94
2c	+0.60	+0.15	-	-	-
2d	+0.76	+0.46	-1.53 ^e	6.02	-1.75
2g	+0.68	+0.20	-	5.60	-0.89
2i	+0.80	+0.54	-2.10	5.99	-1.43
2j	+0.79	+0.40 ^{f,g}	- ^f	5.97	-1.01
2k	+0.91 ^h	+0.58 ^g	-1.99 ^g	6.16	-1.46
2l	+0.90	+0.69 ^g	-1.90 ^g	6.31	-1.63

^a EA is defined here as the free-energy change for the reaction $\text{M} + \text{e}^- \rightarrow \text{M}^-$. ^b EC-type process. ^c An EC-type reduction has been reported for the analogous nonalkylated compound at -3.04 V vs $\text{FeCp}_2^{+/0}$ in DMF.⁷⁴ ^d The greater ease of oxidation of **2a** vs **2b** is consistent with previously reported oxidation potentials of +0.61 and +0.31 V vs $\text{FeCp}_2^{+/0}$ in MeCN for their respective nonalkylated analogues.⁸² ^e An additional, second irreversible molecular reduction is observed at $E_{\text{red}} = \text{ca. } -2.25$ V at 50 mV s⁻¹. ^f Oxidation and reduction previously reported at potentials of +0.40 and -2.61 V, respectively, vs $\text{FeCp}_2^{+/0}$ for the R = $n\text{Bu}$ analogue, in 1:1 $\text{CH}_2\text{Cl}_2/\text{MeCN}$.⁵⁶ ^g These potentials are similar to those recently reported for analogous compounds with R = $n\text{-hexyl}$ and with 3,5-dimethyl substitution of the fused-ring core, also in CH_2Cl_2 .⁶⁰ ^h First of two peak potentials for an irreversible process.

bridged > NAr-bridged > S-bridged > unbridged; this is entirely consistent with our previous study of bis(diarylamino) derivatives of the same four bridging groups, in which, however, the range of potentials was around half that found for the derivatives of **1** due to substantial delocalization of the HOMO onto the diarylamino termini.⁷⁷ The donor ordering $\text{NR} > \text{NAr} > \text{S}$ has also been deduced from the irreversible peak oxidation potentials of dithienopyrroles and dithienothiophene without 2,6-substituents,^{24,76} although calculated gas-phase ionization potentials (vide infra) suggest that **1f'** is more readily oxidized than **1e'**. Moreover, the stronger donor character found for the dithienopyrrole relative to its dithienothiophene analogue is consistent with the relative electron-transfer-donor and π -donor character found for the former moiety in conjugated donor-acceptor polymers.^{33,34}

The 2,6-bis(5-alkyl-2-thienyl)-4H-cyclopenta[2,1-b:3,4-b']bithiophene derivatives, **2**, generally show two successive reversible oxidation processes, the half-wave potentials for which are also reported in Table 1 (see also Figures S4–5 and Table S4, Supporting Information). The half-wave potentials corresponding to molecular oxidations to the radical cations vary by over 0.5 V, with the most readily oxidized compounds being the CR_2 -bridged compounds, **2b** and **2c**, and the least readily oxidized being the SO_2 -bridged compound, **2l**. These potentials show the same trend as those for compounds of type **1**, i.e., that electron-donor strength decreases in the order NAr-bridged > S-bridged > unbridged, but with less variation between extremes, consistent with the significant contribution of the terminal thienyl groups to the HOMO of compounds of type **2**. As shown in Figure 3, the potentials for the fused-ring derivatives correlate well with the Taft parameters, σ_I , for XMe, i.e., with the inductive (σ) electron-withdrawing character of a substituent.^{78–81} This is consistent with the HOMOs shown in Figure 2, in which there is no contribution of the X group. The

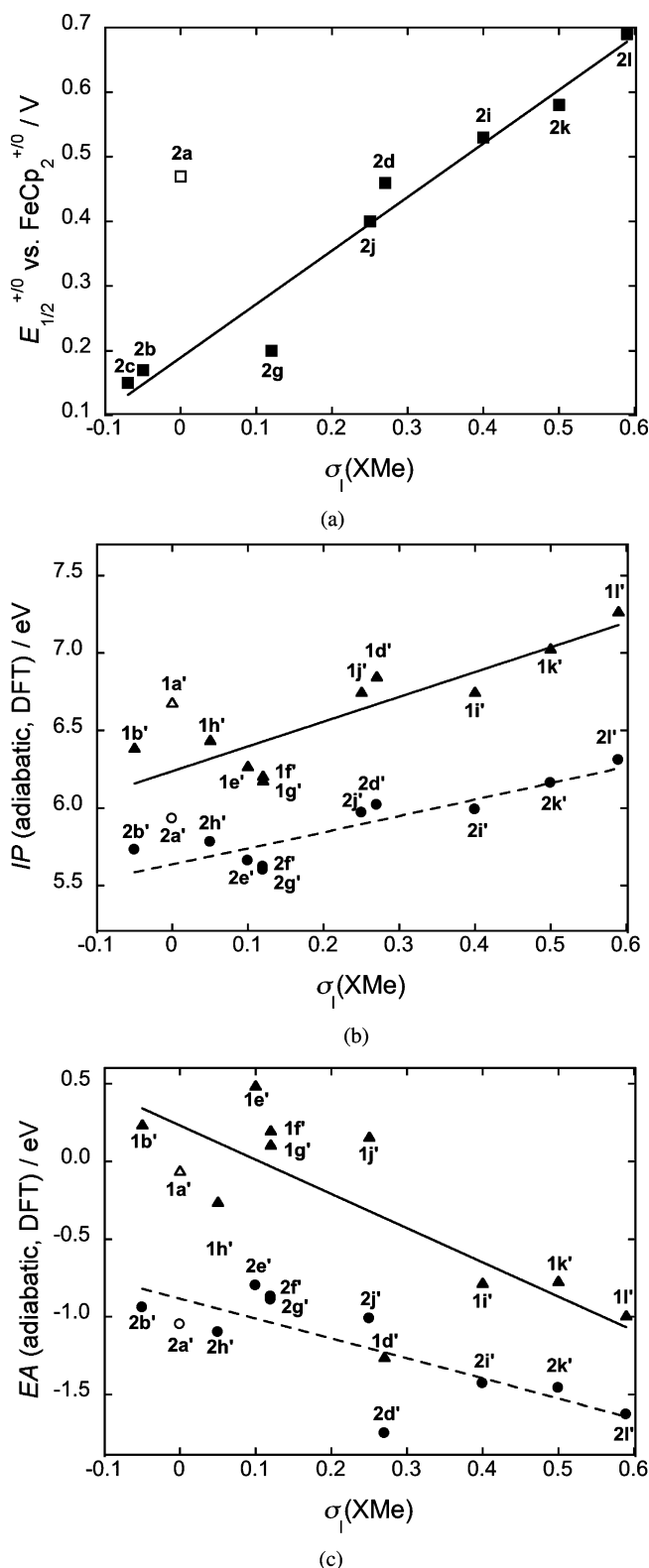


Figure 3. Plots showing variation with the Taft parameter, σ_I , associated with the X group of (a) electrochemical potentials of cyclopentabithiophene derivatives of type **2** and (b and c) DFT-calculated gas-phase adiabatic IPs and EAs of cyclopentabithiophenes of types **1'** (triangles, fit with solid line) and **2'** (circles, fit with broken line). In each case, data for the corresponding unbridged derivative are also shown as an open symbol and are excluded from the linear fit.

potential for the nonfused compound **2a** is also plotted in Figure 3a (at the σ_I value for H, i.e., 0) but is excluded from the fit

TABLE 2: UV–vis, Absorption, and Emission Maxima, Absorptivities, and Oscillator Strengths for the Lowest-Energy Absorptions of Cyclopentabithiophene Derivatives in Dichloromethane with TD-DFT Gas-Phase Values in *Italics*^a

	absorption					emission ^b	
	$\bar{\nu}_{\text{max}}/10^3 \text{ cm}^{-1}$		$\epsilon_{\text{max}}/10^3 \text{ M}^{-1} \text{ cm}^{-1}$		f	$\bar{\nu}_{\text{max}}/10^3 \text{ cm}^{-1}$	Stokes shift/ 10^3 cm^{-1}
1a	31.3	<i>31.5</i>	15.9	0.37	<i>0.55</i>	26.3	5.0
1e^d	32.6	<i>33.8</i>	24.5	0.57	<i>0.58 (0.67)</i>	28.5 ^c	4.1 ^c
1f^d	32.8	<i>31.2</i>	33.1	0.87	<i>0.16 (0.88)</i>	28.5 ^c	4.3 ^c
1j^d	32.8	<i>33.2</i>	20.6	0.49	<i>0.51 (0.60)</i>	28.5 ^c	4.3 ^c
2a	24.8	<i>22.9</i>	36.0	0.83	<i>1.33</i>	21.6	3.2
2b	24.1	<i>22.4</i>	40.5	0.93	<i>1.37</i>	21.3	2.7
2c	23.5	-	45.7	0.90	-	20.8	2.7
2d^e	16.7	<i>14.9</i>	5.0	0.091	<i>0.207</i>	<i>f</i>	<i>f</i>
2e	-	<i>23.4</i>	-	-	<i>1.47</i>	-	-
2f	-	<i>23.3</i>	-	-	<i>1.40</i>	-	-
2g	25.1	<i>23.3</i>	50.1	0.95	<i>1.37</i>	21.9	3.2
2h	-	<i>22.0</i>	-	-	<i>1.11</i>	-	-
2i	22.0	<i>20.8</i>	27.8	0.54	<i>0.90</i>	17.9	4.1
2j	24.5	<i>23.7</i>	51.0	1.1	<i>1.37</i>	22.5	2.0
2k	22.0	<i>21.3</i>	25.3	0.51	<i>0.96</i>	16.6	5.4
2l	22.0	<i>21.0</i>	26.6	0.49	<i>0.95</i>	17.5	4.5

^a Calculated values obtained for the analogous **1'** and **2'** compounds using TD-DFT at the B3LYP/6-31G (d,p) level. ^b Emission maxima refer to the highest-energy maximum in the emission spectrum; the Stokes shift is taken as the energy difference between this maximum and the absorption maximum. ^c Approximate values due to low signal levels.⁸⁵ ^d The experimental values of $\bar{\nu}_{\max}$ and ϵ_{\max} for these compounds refer to the strongest of several peaks arising from vibronic structure and contributions from several excited states, whereas the DFT $\bar{\nu}_{\max}$ values refer to $S_0 \rightarrow S_1$; the DFT oscillator strength for the $S_0 \rightarrow S_1$ transition is given first, with the sum of oscillator strengths for the calculated transitions contributing to the lowest-energy band given in parentheses. ^e The most intense peak in the spectrum of **2d** is observed at $\bar{\nu}_{\max} = 26\,700 \text{ cm}^{-1}$ ($\epsilon_{\max} = 35\,400 \text{ M}^{-1} \text{ cm}^{-1}$); TD-DFT suggests that this should be assigned to $S_0 \rightarrow S_4$ transition, which is the second lowest-energy transition with significant oscillator strength and for which values of $\bar{\nu}_{\max} = 26\,100 \text{ cm}^{-1}$ and $f = 1.02$ are calculated. ^f No fluorescence observed.

since the twist around the central thiophene–thiophene bond is anticipated to affect $E_{1/2}^{+/0}$ significantly; indeed, the plot shows that **2a** is considerably less readily oxidized than fused species with X groups having either small positive or negative values of σ_I . Thus, the *greater* ease of oxidation of, for example, the dithienothiophene derivative, **2j**, relative to that of **2a** can be attributed to the planarization effect of the bridging sulfur atom, rather than to its electronic effects, which, for this example, have an opposing effect on the potential.

Figure 3 also shows that the DFT-calculated gas-phase adiabatic ionization potentials (IPs) for the fused-ring members of series **1** and **2** also correlate reasonably well with $\sigma_I(\text{XMe})$, although the calculated values suggest that the dithienopyrrole derivatives should be more readily oxidized than the corresponding CR₂-bridged cyclopentabithiophenes (as is also suggested by irreversible peak potentials for nonalkylated analogues of **1b** and **1e**⁷⁶), whereas the electrochemical data indicate the opposite is true for compounds of type **2**, at least in solution. A similar dependence is observed for the DFT-calculated HOMO energies (see Table S1, Supporting Information). The IPs show a somewhat steeper dependence for series **1** than **2**, presumably due to the greater concentration of the relevant molecular orbitals on the fused-ring core in the former series.

For the compounds in which X is strongly electron-withdrawing, either in an inductive or resonance sense (X = CO, P(O)Ph, SO, SO₂; **2d**, **2i**, **2k**, **2l**, respectively), reversible reductions are also observed, with **2d** being the most readily reduced. The ordering of reduction potentials for these compounds is consistent with DFT estimates of gas-phase adiabatic electron affinities (EA, Table 1, Figure 3c) and LUMO energies (see Supporting Information, Table S1). Moreover, the reductions of the isolated cores 4*H*-cyclopenta[2,1-*b*:3,4-*b'*]bithiophene-4-one and dithieno[3,2-*b*:2',3'-*d*]thiophene 4,4-dioxide have previously been reported at -1.62 and -2.00 V, respectively, vs $\text{FcCp}_2^{+/0}$ in DMF;^{83,84} the similarity of these potentials to those of the respective members of the **2** series is consistent

with the large LUMO coefficients on the fused-ring cores of **2d** and **2l** (Figure 2). Values of $E_{1/2}^{0/-}$, EA, and LUMO energy correlate much less well with $\sigma_I(\text{XMe})$ than values of $E_{1/2}^{+/0}$, IP, and HOMO energy, indicating that these quantities do not depend only upon the inductive properties of X. Indeed, the moderate σ_I group CO results in the most readily reduced compounds. This is consistent with the LUMOs shown in Figures 3 and S2, which show varying π -contributions by the X groups, with a particularly significant stabilizing contribution being evident in the case of X = CO (**1d'**, **2d'**). The deviation of the calculated EAs of X = NAr, NR, and S derivatives (**1e–g'**, **1j'**, **2e–g'**, **2j'**) from the best fit in Figure 3c is also consistent with destabilizing contributions of these π -donor substituents to the LUMOs evident in Figures 3 and S2.

Optical Properties. The UV–vis, absorption, and fluorescence spectra of **1a**, **1e**, **1f**, and **1j** were recorded in dichloromethane and are shown in Figures 5a and S8, respectively, while absorption maxima for a greater range of compounds of type **1** were obtained from TD-DFT calculations. Consistent with previous reports for their nonalkylated analogues,^{24,26,56,76} the spectra of these fused-ring systems exhibit a vibronic structure not found for their bithiophene analogue and are also hypsochromically shifted with respect to that of **1a**. The 2,6-alkylation of **1a**, **1e**, **1f**, and **1j** results in slight bathochromic shifts of both absorption and fluorescence⁸⁵ maxima relative to those of their respective nonalkylated analogues.^{24,26,56,76,86,87} The TD-DFT calculations indicate that in each case the $S_0 \rightarrow S_1$ transition is predominantly HOMO-to-LUMO in character. The calculations also indicate that in a few of the compounds—**1e'–g'** and **1j'**—other transitions lie only slightly higher ($<5000 \text{ cm}^{-1}$) in energy than $S_0 \rightarrow S_1$ and also exhibit significant oscillator strengths, f . Thus, the calculations suggest that several excited states contribute to the experimentally observed low-energy absorption bands of **1e**, **1f**, and **1j**; indeed, as shown in Table 2, experimental values of the oscillator strengths for the low-energy band, of **1f** in particular, are in much better

agreement with theory when the calculated values of f are summed for all the transitions predicted within an energy of $S_0 \rightarrow S_1$ corresponding to the experimental bandwidth (see Supporting Information, Table S2, for individual calculated transition energies and oscillator strengths). The aforementioned hypsochromic shift of the experimentally examined fused-ring systems relative to the bithiophene derivative is reproduced by TD-DFT $S_0 \rightarrow S_1$ transition energies for $X = \text{NR}$ and S examples (**1e'**, **1j'**, respectively), although that for the $X = \text{NAr}$ example **1f'** is predicted to be slightly bathochromically shifted vs **1a'**. Planarization of the ring system would be expected to result in a bathochromic shift; indeed, the TD-DFT $S_0 \rightarrow S_1$ absorption maximum for the $X = \text{CH}_2$ system (**1b'**), in which the X group does not contribute directly to the frontier orbitals, is at slightly lower energy than that of **1a'**, consistent with experimental data for nonalkylated analogues.^{76,88} The hypsochromic shift is, therefore, presumably attributable to the destabilizing contribution of the $p\pi$ -orbitals of the X heteroatoms to the LUMOs (vide supra), as previously recognized by Zhang and Matzger in the context of comparing 2-(2-thienyl)dithieno[3,2-*b*:2',3'-*d*]thiophene and its unbridged terthiophene analogue.⁴⁹ Moreover, the calculated absorption maxima for the compounds in which the X groups provide stabilizing contributions to the LUMO (**1d'**, **1h'**, **1i'**, **1k'**, **1l'**) are more strongly bathochromically shifted than that of **1b'** (see Table S2, Supporting Information, for full data); this is consistent with previous reports of absorption maxima for dithieno[3,2-*b*:2',3'-*d*]thiophene 4-oxide and 4,4-dioxide derivatives (350–370 nm)^{61,73} and for 4*H*-cyclopenta[2,1-*b*:3,4-*b'*]bithiophene-4-one (weak absorption at 475 nm).¹⁵

UV–vis absorption spectra were measured for a variety of compounds of series **2**; representative examples are shown in Figure 4b (spectra for the remaining compounds are shown in the Supporting Information, Figure S6). The spectra fall into three distinct groups. First, the lowest-energy absorptions of $X = \text{CH}_2$, NAr , and S examples (**2b**, **2g**, **2j**) exhibit strong absorption maxima at energy similar to that of their nonfused bithiophene analogue (**2a**) but which show some poorly resolved vibronic structure. As expected, and consistent with data for nonalkylated analogues,^{5,8,82,89} the methylene bridge of **2b** leads to a slight bathochromic shift relative to **2a**, while the similar absorption maxima found for **2a**, **2g**, and **2j** presumably reflect the interplay of planarization and π donation effects discussed for the **1** series. The absorption maxima for the compounds in this group are very similar to those previously reported for close analogues with different or absent alkyl substituents.^{5,8,26,52,56,60,82,86,89} In general, the presence of the terminal alkyl groups seems to result in a slight bathochromic shift, although the maximum for **2g** is at higher energy than that reported for an analogue with $X = \text{N}(n\text{-C}_8\text{H}_{17})$ and $R = \text{H}$.²⁶ The second group consists of **2i**, **2k**, and **2l**—compounds in which $\text{P}-\text{O}$ or $\text{S}-\text{O}$ σ^* orbitals stabilize the LUMO: all show structureless absorptions that are bathochromically shifted by ca. 50 nm relative to those of the first group and that are somewhat weaker, with additional absorptions of moderate strength present at ca. 330 nm. Not surprisingly, the absorption maximum of **2l** is significantly bathochromically shifted relative to that of a previously reported analogue, 2,6-di(3-methylthien-2-yl)-3,5-dimethyldithieno[3,2-*b*:2',3'-*d*]thiophene 4,4-dioxide (25 000 cm^{-1}), in which the alkylation pattern leads to a large dihedral angle between the thienyl rings and the core,⁶³ but **2k** and **2l** show absorption maxima similar to analogues with $R = n\text{-hexyl}$ and with 3,5-dimethyl substitution of the fused core.⁶⁰ A little more surprisingly, the absorption maximum of **2i** ($X = \text{P}(\text{O})\text{Ph}$) is somewhat

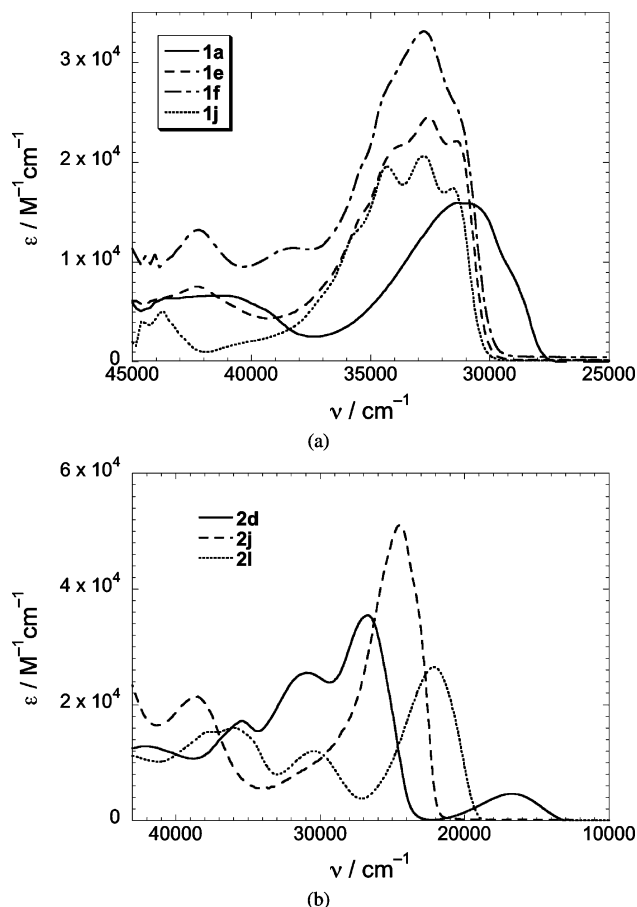


Figure 4. UV–vis absorption spectra of cyclopentabithiophene derivatives of types (a) **1** and (b) **2** in dichloromethane. The three spectra shown in (b) represent the three groups discussed in the text.

hypsochromically shifted relative to that reported from its nonalkylated ($R = \text{H}$) analogue in the same solvent (20 600 cm^{-1}).³⁹ Finally, the $X = \text{CO}$ derivative, **2d**, in which the LUMO is largely localized on the fused-ring core (vide supra), shows yet a different type of spectrum characterized by a weak low-energy band at ca. 600 nm, with more intense bands at somewhat higher energy than the lowest-energy band of **2a**; a similar spectrum with an absorption maximum of 545 nm has previously been reported for a similar molecule in which $R = \text{C}(\text{O})-n\text{-C}_6\text{F}_{13}$.^{11,18} Broadly similar spectra are observed for conjugated polymers based on 4*H*-cyclopenta[2,1-*b*:3,4-*b'*]bithiophene-4-one¹⁵ and for simple derivatives of the same core, including the 2,6-bis(trimethylsilyl) and 2,6-diiodo derivatives used as intermediates in the synthesis of **2d** (see Supporting Information, Figure S7). The absorption maxima and oscillator strengths obtained from TD-DFT calculations are broadly consistent with these three types of spectral behavior. In each case, the calculations indicate that the observed low-energy absorption band corresponds to the transition to the first excited state, which can be well-described as HOMO-to-LUMO excitation, and which, in contrast to a situation for some compounds of type **1**, is well separated in energy ($>5000 \text{ cm}^{-1}$) from transitions to higher excited states. Accordingly, the differences in energies and oscillator strengths of the low-energy bands can be rationalized in terms of the energies (see Table S1) and spatial characteristics (Figures 3 and S2) of the HOMOs and LUMOs: the increased stabilization of the LUMO by interactions with the X groups, which is responsible for lowering the transition energy, is accompanied by increased localization of the LUMO onto the fused-ring core and toward the X portion of the core,

and therefore leads to decreased contributions to the transition dipole moment from the terminal thienyl groups and, hence, to weaker transitions.

Fluorescence spectra for compounds of series **2** (recorded in dichloromethane) fall into the same three groups as the absorption spectra (see Supporting Information, Figure S8). The $X = \text{CH}_2$, CR_2 , NAr , and S examples (**2b**, **2c**, **2g**, **2j**) exhibit emissions with resolved vibronic structure ($\Delta\nu \sim 1100\text{--}1300\text{ cm}^{-1}$) similar to that of the nonfused bithiophene-cored compound (**2a**); this is consistent with previous reports for quaterthiophenes and their fused analogues,⁵ the increased vibronic structure relative to that in the absorption spectra being consistent with increased planarity of the terminal thienyl groups with the core in the excited states.⁹⁰ Stokes shifts (estimated as the energy difference between the maximum of the broad absorption peak and the highest-energy maximum in the emission spectrum) vary from just below 2000 cm^{-1} to just over 3000 cm^{-1} . Emission maxima for **2a**, **2b**, **2j**, and **2g** are very similar to previously reported values for close analogues.^{5,8,26,52,56,60,82,86,89} The $\text{P}(\text{O})\text{Ph}$, SO , and SO_2 compounds (**2i**, **2k**, **2l**) all show structureless emissions and larger Stokes shifts ($>4000\text{ cm}^{-1}$); these are consistent with the corresponding excited states having more pronounced quadrupolar charge-transfer character, as suggested by the absorption spectra and the frontier molecular orbitals (vide supra). As with the absorption maxima, the emission maximum for **2i** is at somewhat higher energy than that of its nonalkylated analogue ($18\,300\text{ cm}^{-1}$),³⁹ while those for **2k** and **2l** are similar to those of analogues with $R = n\text{-hexyl}$ and with 3,5-dimethyl substitution of the fused core.⁶⁰ Finally, no emission was observed for the CO compound, **2b**, in which the orbitals (Figure 2) and absorption spectrum (Figure 4b) suggest the most pronounced charge-transfer character for any of the compounds considered here.

Optical and Electron Spin Resonance Spectra of Radical Cations. Many 4*H*-cyclopenta[2,1-*b*:3,4-*b'*]bithiophene derivatives are of interest as hole-transport materials; accordingly, the corresponding radical cations, which act as the charge-carrying species, are of relevance. Visible/near-infrared (vis–NIR) and electron spin resonance (ESR) spectra were acquired in solution for some examples of the radical cations of compounds of types **1** and **2**; the cations were generated from dichloromethane solutions of the neutral compounds using substoichiometric tris(4-bromophenyl)aminium hexachloroantimonate ($E_{1/2}^{+/0} = 0.70\text{ V}$ vs $\text{FeCp}_2^{+/0}$) as an oxidant.^{91,92}

The electrochemistry of **1a** and **1j** (vide supra) indicates that the corresponding radical cations are not stable; indeed, the vis–NIR and ESR spectra of chemically oxidized samples change rapidly over time. However, oxidation of the dithienopyrrole derivatives, **1e** and **1f**, gives rise to vis–NIR and ESR spectra that are reproducible over multiple scans, indicating lifetimes of 10+ min. The visible spectra of both show vibronically structured bands ($\Delta\nu \sim 1300\text{ cm}^{-1}$) with maxima at ca. 580 nm (Figure 5a shows the spectrum for **1e**^{•+}, while that for **1f**^{•+} is shown in the Supporting Information, Figure S9), with an additional band at ca. 395 nm; previously, absorption maxima of ca. 550 and 380 nm have been observed for the radical cation of the unsubstituted dithieno[3,2-*b*:2',3'-*d*]pyrrole core (i.e., $X = \text{NH}$, $R = \text{H}$) in chlorobutane at 77 K.⁷⁶ Table 3 compares the experimental results with those from TD-DFT calculations. The electronic structure calculations indicate that the transition to the first excited state ($D_0 \rightarrow D_1$) for most compounds can be described as predominantly (SOMO-1)-to-SOMO in character, with these orbitals closely corre-

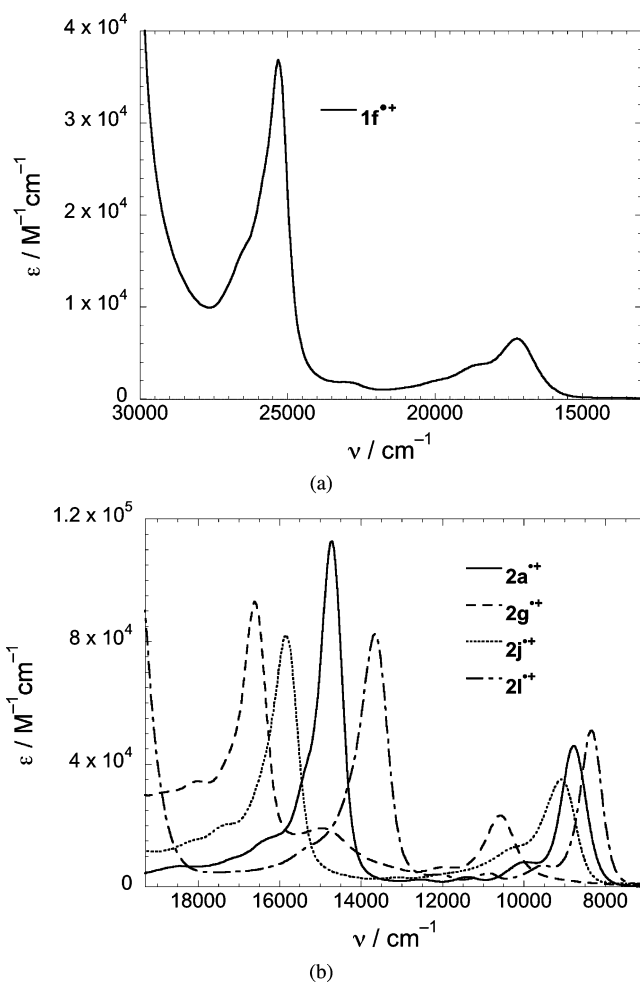


Figure 5. Vis–NIR absorption spectra of the radical cations of cyclopentabithiophene derivatives of types (a) **1** and (b) **2** in dichloromethane. The onsets of strong absorption seen at the high-energy edges of the spectra for **1f**^{•+} and **2l**^{•+} are due to the presence of large excesses of the respective neutral species.

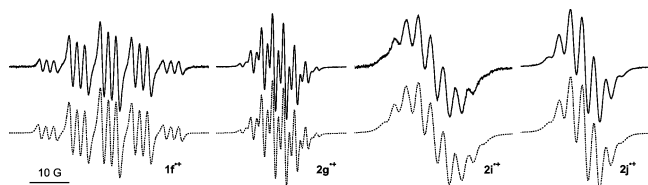
sponding to the HOMO-1 and HOMO, respectively, of the neutral compounds (although for **1d**^{•+}, SOMO-to-LUMO is a more important configuration). In all cases, the oscillator strength for the $D_0 \rightarrow D_1$ transition is calculated to be extremely small (0.0000–0.0034), suggesting that the experimentally observed bands at ca. 580 nm are due to transitions to higher excited states ($D_0 \rightarrow D_3$ and $D_0 \rightarrow D_5$ for **1e**^{•+} and **1f**^{•+}, respectively).⁹³ The TD-DFT gas-phase absorption maxima are somewhat overestimated compared to the experimental solution values. TD-DFT results for the other **1**^{•+} cations (see Supporting Information, Table S3) predict that the lowest-energy moderately intense ($f > 0.01$) absorption maxima for most of the chromophores fall in the range $17\,000\text{--}19\,800\text{ cm}^{-1}$ (506–565 nm), with the exception of the $X = \text{PPh}$ and $\text{P}(\text{O})\text{Ph}$ examples (**1h**^{•+} and **1i**^{•+}), which show significantly lower-energy bands ($12\,400$ and $11\,800\text{ cm}^{-1}$, respectively). The calculated value for the dithienothiophene derivative **1j**^{•+} ($18\,500\text{ cm}^{-1}$) is, allowing for a comparable margin of overestimation to that seen for **1e**^{•+} and **1f**^{•+}, broadly consistent with values previously reported for the radical cation of unsubstituted dithieno[3,2-*b*:2',3'-*d*]thiophene, generated in various media at 77 K ($16\,800\text{ cm}^{-1}$).^{76,94}

The **2**^{•+} radical cations show vibronically structured absorptions with moderate intensity in the near-IR range with maxima at wavelengths between ca. 900 and 1200 nm, with additional

TABLE 3: Vis–NIR Absorption Maxima, Absorptivities, and Transition Dipole Moments for the Lowest-Energy Absorptions of Cyclopentabithiophene-Based Radical Cations in Dichloromethane with TD-DFT Gas-Phase Values in Italics^a

	$\bar{\nu}_{\max}/10^3 \text{ cm}^{-1}$	$\epsilon_{\max}/10^3 \text{ M}^{-1} \text{ cm}^{-1}$	f	calculated transition
1e⁺	17.3	19.8	8.0	0.11 0.068 D ₀ →D ₃
1f⁺	17.2	19.8	6.6	0.09 0.068 D ₀ →D ₅
2a⁺	8.79	10.0	46	0.20 0.19 D ₀ →D ₁
2b⁺	9.86	10.8	52	0.12 0.12 D ₀ →D ₁
2c⁺	9.92	-	49	0.11 - -
2d⁺	9.03	9.17	29	0.16 0.013 D ₀ →D ₁
2e⁺	-	10.9	-	- 0.12 D ₀ →D ₁
2f⁺	-	11.7	-	- 0.15 D ₀ →D ₂
2g⁺	10.6	11.4	23	0.15 0.17 D ₀ →D ₂
2h⁺	-	10.6	-	- 0.15 D ₀ →D ₁
2i⁺	8.75	10.1	42	0.18 0.11 D ₀ →D ₁
2j⁺	9.07	10.5	35	0.23 0.21 D ₀ →D ₁
2k⁺	8.75	10.1	44	0.21 0.22 D ₀ →D ₁
2l⁺	8.34	9.88	51	0.19 0.25 D ₀ →D ₁

^a Experimental values are the lowest-lying clearly identifiable maxima; calculated values were obtained using TD-DFT at the B3LYP/6-31G(d,p) level for the analogous **1⁺** and **2⁺** cations and refer to the transitions believed to correspond to the experimental peaks.

**Figure 6.** ESR spectra of radical cations of some cyclopentabithiophene derivatives in dichloromethane with simulations used to obtain the coupling constants reported in Table 4 shown as dashed lines. The horizontal scale is the same for all four plots.

strong features in the 600–800 nm range; representative examples are shown in Figure 5b with the remainder appearing in the Supporting Information (Figure S11) and results being summarized in Table 3. Both high- and low-energy absorptions for the nonfused quaterthiophene derivative, **2a⁺**, (14 700 and 8770 cm⁻¹) occur at energies similar to those of its nonalkylated analogue (15 500 and 7900 cm⁻¹)⁹⁵ and of other substituted quaterthiophenes (14 700–15 000 and 8700–8900 cm⁻¹)^{96,97} in

the same solvent.⁹⁸ The absorptions for **2i⁺** (X = P(O)Ph) are seen at energies fairly similar to those reported for its nonalkylated analogue in chlorobutane at 100 K (15 900 and 9910 cm⁻¹);³⁸ however, the calculated oscillator strengths for the low-energy bands X = PPh and P(O)Ph derivatives, **2h⁺** and **2i⁺**, are similar, while values reported for their nonalkylated analogues differ by a factor of ca. 6.³⁸

In all cases, TD-DFT calculations show that the D₀→D₁ transition has significant (SOMO-1)-to-SOMO character. For most compounds, the computed oscillator strengths for these transitions are of similar magnitude to the experimental values, while the transition energies are somewhat higher than the experimental maxima. However, for **2f⁺** and **2g⁺** (X = NAr), calculations indicate rather weak D₀→D₁ transitions ($f = 0.037$ and 0.0050, respectively), suggesting that the lowest-energy absorption maximum seen for **2g⁺** is due to a transition to the second excited state (D₀→D₂). The computed oscillator strength and transition energy agree well with the experimental data; moreover, a weak low-energy tail evident in Figure 5b presumably corresponds to the weak D₀→D₁ transition. The TD-DFT results do not model the spectrum of **2d⁺** (X = CO) so well; the observed transition is close in energy to that calculated for D₀→D₁ but is considerably stronger than predicted, while the D₀→D₂ transition is calculated to occur at much higher energy (13 600 cm⁻¹) and with a much greater oscillator strength (0.82). Although a simple rationalization of the optical behavior of these radical cations in terms of the molecular orbital structure is hampered by significant configuration interaction, the localization of the **2g⁺** SOMO-1 (similar to the HOMO-1 of both **2g'** and **2f**, shown in Figure 2b and Figure S2 (Supporting Information), respectively on the fused-ring core and the *N*-aryl substituent may contribute to the low oscillator strength for the D₀→D₁ transition of **2g⁺**.

ESR spectra of **1⁺** and **2⁺** cations show well-resolved hyperfine coupling patterns; representative examples are shown in Figure 6, with the remaining spectra being shown in the Supporting Information (Figure S12). Experimental hyperfine coupling constants were extracted by simulation using WinSim^{99,100} and assigned with the help of DFT calculations. As shown in Table 4, the spectra of **1e⁺** and **1f⁺** were both satisfactorily simulated taking into account coupling to four equivalent $I = 1/2$ nuclei, assigned to the ¹H nuclei of the α-CH₂ groups of the terminal *n*-butyl substituents and to a single $I = 1$ nucleus, i.e., the ¹⁴N of the X group; coupling to the 3,5-protons was

TABLE 4: Experimental and DFT (Italics) Values of Hyperfine Coupling Constants^a (G) for Cyclopentabithiophene Radical Cations.

compound	X nuclei	A_X	$A_{H(\alpha-CH_2)}^b$		$A_{H(\text{core-3,5})}$		$A_{H(\text{thienyl-1,3'})}$	
1e⁺	1 × ¹⁴ N	1.83	<i>−1.80</i>	7.50	9.93	-	0.85	-
1f⁺	1 × ¹⁴ N	1.93	<i>−1.79</i>	7.08	9.89 ^c	-	0.92 ^c	-
2a⁺d	2 × ¹ H	3.43	<i>−2.43</i>	2.36	4.40	-	<i>−1.06</i>	0.78 <i>−2.86</i>
2d⁺	-	-	-	2.90	4.72	-	<i>−0.15</i>	2.70 <i>−3.09</i>
2g⁺	1 × ¹⁴ N	1.46	<i>−1.20</i>	2.79	4.31 ^c	-	0.29 ^c	2.56 <i>−3.19^c</i>
2i⁺	1 × ³¹ P	5.93	<i>−4.53</i>	2.63	4.55	-	<i>−0.34</i>	3.71 <i>−3.02</i>
2j⁺	-	-	-	3.30	4.60	-	0.47	2.63 <i>−3.00</i>
2k⁺	-	-	-	3.17	4.74	-	<i>−0.51</i>	2.21 <i>−2.97</i>
2l⁺d	-	-	-	3.17	4.85	1.06	<i>−0.68</i>	2.66 <i>−2.89</i>

^a Experimental values are moduli (|A|). Calculated values are isotropic Fermi contact couplings for the corresponding **1⁺** and **2⁺** species obtained at the open-shell B3LYP/6-31G(d,p) DFT level with both sign and magnitude. ^b Calculated values given here are the average of coupling constants for the three Me ¹H nuclei in the lowest-energy calculated conformer. ^c Due to the orientation of the Ar substituent in the minimized conformer, the low symmetry of modeled structures means that two different values are obtained for each of these parameters. The number quoted is an average. ^d Experimental values and their assignment uncertain due to several alternative comparable fits being possible. Similar theoretical values have previously been obtained for **2a⁺** using RHF-INDO/S calculations, while an experimental spectrum of **2a⁺** obtained in trifluoroacetic acid at 258 K showed better resolution than our spectrum of **2a** and was simulated using a coupling to the methyl protons of 3.41 G and to three pairs of equivalent protons with coupling constants of 2.56, 2.55, and 1.09 G.¹⁰¹

calculated to be small, and inclusion in the simulation did not result in any significant improvement to the fit. In the case of 2^{*+} cations, spectra were generally satisfactorily fitted considering coupling to the four equivalent $\alpha\text{-CH}_2$ ^1H nuclei, two equivalent ^1H nuclei in the 3-positions of the two thienyl substituents (coupling to the ^1H 's in the 4-positions of the thienyl groups are calculated to be very small), and nuclei associated with the X group. The coupling constants extracted from the simulations are in reasonable agreement with those obtained from DFT calculations, suggesting that the calculations describe well the spin distribution in molecules of this type (vide infra). The largest discrepancies are in the value of $A_{\text{H}(\alpha\text{-CH}_2)}$ and for $2\mathbf{a}^{*+}$; the former discrepancy is likely to be partly due to the strong dependence of each coupling constant on the angle between the C–H bond in question and the plane of the aromatic ring and to the fact that only a single rotational conformer of the Me groups was modeled.

The calculated spin density in the 1^{*+} cations is, as expected, overwhelmingly located on the fused-ring core, with only 2–3% extending onto the 2,6-methyl groups. In the case of the 2^{*+} series, 52–59% of the spin density is found on the core, with 40–47% on the thienyl groups and ca. 1% on the Me groups. The distribution over the entire π -system is consistent with the HOMOs of the neutral $2'$ molecules (corresponding to the SOMOs of the radical cations) shown in Figure 2. The dithienopyrrole derivatives are calculated to exhibit the greatest spin density on the core, while the lowest core spin density is anticipated for the dithienothiophene dioxide derivative ($2\mathbf{l}$), in which X is most strongly inductively withdrawing. However, the spin distributions (see Supporting Information, Table S5) do not correlate as closely with $\sigma_{\text{I}}(\text{XMe})$ values as do the electrochemical potentials and calculated IPs (vide supra).

Summary

The electronic and optical properties of 4*H*-cyclopenta[2,1-*b*:3,4-*b'*]bithiophene derivatives can be significantly modified by variation of the bridging group, X, in the 4-position. The bridging atom lies on a nodal plane of the highest occupied molecular orbital; thus, while a methylene bridge results in increased ease of oxidation relative to bithiophene due to planarization of the core, variation in ease of oxidation between compounds with different bridging groups (X) correlates well with the inductive electron-withdrawing/-donating properties of the bridging group. In the case of 2,6-bis(5-alkyl-2-thienyl) derivatives, the radical cations are moderately stable in solution; comparison of experimental and DFT hyperfine coupling constants suggests that the hole in these species is delocalized over both core and terminal thienyl groups, with only minor variation in this distribution with variation of the bridging group, consistent with the DFT HOMOs. In contrast, the lowest unoccupied orbital is influenced by both inductive and π donor/acceptor properties of the group; accordingly, the example with the strongest π -accepting bridge examined (X = CO) results in the most readily reduced compounds and in the weakest and lowest-energy visible absorptions. On the other hand, π -donor X groups destabilize the LUMO, leading to the compounds with the highest-energy absorptions. The radical cations of the 2,6-bis(5-alkyl-2-thienyl)derivatives all show two reasonably strong absorptions in the visible and/or near-IR region; the energies of these features vary significantly with X.

Acknowledgment. This work was supported by the National Science Foundation through the Science and Technology Center Program (DMR-0120967) and CRIF (CHE-0443564) Programs

and through a Graduate Research Fellowship to SAO. We also thank Robert Twieg, in whose laboratory 2-tri-*n*-butylstannyl-5-alkylthiophene intermediates were synthesized by YAG, and Mariacristina Rumi for help with fluorescence measurements.

Supporting Information Available: Synthetic procedures and characterizing data for experimentally studied compounds; details of quantum-chemical calculations; figures showing frontier MOs for all computationally investigated compounds; tables of calculated HOMO and LUMO energies, IPs, EAs, neutral and radical-cation absorption data, ESR hyperfine coupling constants, and spin distribution; figures showing UV–vis absorption and fluorescence spectra, radical-cation vis–NIR and ESR spectra not shown in the main body of the paper. This material is available free of charge via the Internet at <http://pubs.acs.org>.

References and Notes

- (1) Li, Y.; Zou, Y. *Adv. Mater.* **2008**, *20*, 2952, and references therein.
- (2) Mishra, A.; Ma, C.-Q.; Bäuerle, P. *Chem. Rev.* **2009**, *109*, 1141, and references therein.
- (3) Cheng, Y.-J.; Yang, S.-H.; Hsu, C.-S. *Chem. Rev.* **2009**, *109*, 5868, and references therein.
- (4) *Handbook of Thiophene-Based Materials: Applications in Organic Electronics and Photonics*; Perepichka, I. F., Perepichka, D. F., Eds.; Wiley: New York, 2009.
- (5) Benincori, T.; Bongiovanni, G.; Botta, C.; Cerullo, G.; Lanzani, G.; Mura, A.; Rossi, L.; Sannicolò, F.; Tubino, R. *Phys. Rev. B* **1998**, *58*, 9082.
- (6) Zotti, G.; Destri, S.; Porzio, W.; Pasini, M.; Rizzo, S.; Benincori, T. *Macromol. Chem. Phys.* **2001**, *202*, 3049.
- (7) Knapfer, M.; Fink, J.; Zoyer, E.; Leising, G.; Fichou, D. *Chem. Phys. Lett.* **2000**, *318*, 585.
- (8) Benincori, T.; Bongiovanni, G.; Botta, C.; Cerullo, G.; Lanzani, G.; Mura, A.; Sannicolò, F.; Rossi, L.; Tubino, R. *Synth. Met.* **1999**, *101*, 522.
- (9) Zotti, G.; Shiavon, G.; Berlin, A.; Fontana, G.; Pagani, G. *Macromolecules* **1997**, *27*, 1938.
- (10) Benincori, T.; Consonni, V.; Gramatica, P.; Pilati, T.; Rizzo, S.; Sannicolò, F.; Todeschini, R.; Zotti, G. *Chem. Mater.* **2001**, *13*, 1665.
- (11) Yoon, M.-H.; DiBenedetto, S.; Russel, M. T.; Fachetti, A.; Marks, T. J. *Chem. Mater.* **2007**, *19*, 4864.
- (12) Ie, Y.; Nitani, M.; Ishikawa, M.; Nakayama, K.; Tada, H.; Kaneda, T.; Aso, Y. *Org. Lett.* **2007**, *9*, 2115.
- (13) Zhang, M.; Tsao, H. N.; Pisula, W.; Yang, C. D.; Mishra, A. K.; Müllen, K. *J. Am. Chem. Soc.* **2007**, *129*, 3472.
- (14) Ferraris, J. P.; Lambert, T. L. *J. Chem. Soc., Chem. Commun.* **1991**, 1268.
- (15) Ferraris, J. P.; Lambert, T. L. *J. Chem. Soc., Chem. Commun.* **1991**, 752.
- (16) Ferraris, J. P.; Henderson, C.; Torres, D.; Meeker, D. *Synth. Met.* **1995**, *72*, 147.
- (17) Coppo, P.; Adams, H.; Cupertino, D. C.; Yeates, S. G.; Turner, M. L. *Chem. Commun.* **2003**, 2548.
- (18) Yoon, M.-H.; DiBenedetto, S.; Fachetti, A.; Marks, T. J. *J. Am. Chem. Soc.* **2005**, *127*, 1348.
- (19) Yen, W.-C.; Pal, B.; Yang, J.-S.; Hung, Y.-C.; Lin, S.-T.; Chao, C.-Y.; Su, W.-F. *J. Polym. Sci., Part A* **2009**, *47*, 5044.
- (20) Kim, S.; Song, S.-H.; Kang, S. O.; Ko, J. *Chem. Commun.* **2004**, 68.
- (21) Ohshita, J.; Kai, H.; Takata, A.; Iida, T.; Kunai, A.; Ohta, N.; Komaguchi, K.; Shiotani, M.; Adachi, A.; Sakamaki, K.; Okita, K. *Organometallics* **2001**, *20*, 4800.
- (22) Kunai, A.; Ohshita, J.; Iida, T.; Kanehara, K.; Adachi, A.; Okita, K. *Synth. Met.* **2003**, *137*, 1007.
- (23) Zhan, X.; Barlow, S.; Marder, S. R. *Chem. Commun.* **2009**, 1948, and references therein.
- (24) Ogawa, K.; Rasmussen, S. *J. Org. Chem.* **2003**, *68*, 2921.
- (25) Ogawa, K.; Rasmussen, S. C. *Macromolecules* **2006**, *39*, 1771.
- (26) Radke, K. R.; Ogawa, K.; Rasmussen, S. C. *Org. Lett.* **2005**, *7*, 5253.
- (27) Koeckelberghs, G.; Cremer, L. D.; Persoons, A.; Verbiest, T. *Macromolecules* **2007**, *40*, 4173.
- (28) Liu, J. Y.; Zhang, R.; Sauv  , G.; Kowalewski, T.; McCullough, R. D. *J. Am. Chem. Soc.* **2008**, *130*, 13167.
- (29) Zhou, E. J.; Nakamura, M.; Nishizawa, T.; Zhang, Y.; Wei, Q. S.; Tajima, K.; Yang, C. H.; Hashimoto, K. *Macromolecules* **2008**, *41*, 8302.

- (30) De Cremer, L.; Vandeleene, S.; Maesen, M.; Verbiest, T.; Koeckelberghs, G. *Macromolecules* **2008**, *41*, 591.
- (31) Yue, W.; Zhao, Y.; Shao, S.; Tian, H.; Xie, Z.; Geng, Y.; Wang, F. *J. Mater. Chem.* **2009**, *19*, 2199.
- (32) Steckler, T. T.; Zhang, X.; Hwang, J.; Honeyager, R.; Ohira, S.; Zhang, X.-H.; Grant, A.; Ellinger, S.; Odom, S. A.; Sweat, D.; Tanner, D. B.; Rinzler, A. G.; Barlow, S.; Brédas, J. L.; Kippelen, B.; Marder, S. R.; Reynolds, J. R. *J. Am. Chem. Soc.* **2009**, *131*, 2824.
- (33) Zhang, S.; Guo, Y.; Fan, H.; Liu, Y.; Chen, H.-Y.; Yang, G.; Zhan, X.; Liu, Y.; Li, Y.; Yang, Y. *J. Polym. Sci., Part A* **2009**, *47*, 5498.
- (34) Zhan, X.; Tan, Z.; Zhou, E.; Li, Y.; Misra, R.; Grant, A.; Domercq, B.; Zhang, X.; An, Z.; Zhang, X.; Barlow, S.; Kippelen, B.; Marder, S. R. *J. Mater. Chem.* **2009**, *19*, 5794.
- (35) Zhang, X.; Steckler, T. T.; Dasari, R. R.; Ohira, S.; Potscavage, W. J.; Tiwari, S. P.; Coppée, S.; Ellinger, S.; Barlow, S.; Brédas, J.-L.; Kippelen, B.; Reynolds, J. R.; Marder, S. R. *J. Mater. Chem.* **2010**, *20*, 123.
- (36) Baumgartner, T.; Neumann, T.; Wirges, B. *Angew. Chem., Int. Ed.* **2004**, *43*, 6197.
- (37) Baumgartner, T.; Bergmans, W.; Kárpáti, T.; Neumann, T.; Nieger, M.; Nyulász, L. *Chem.—Eur. J.* **2005**, *11*, 4687.
- (38) Acharya, A.; Koizumi, Y.; Seki, S.; Saeki, A.; Tagawa, S.; Ie, Y.; Aso, Y. *J. Photochem. Photobiol. A* **2005**, *173*, 161.
- (39) Dienes, Y.; Durben, S.; Karpati, T.; Neumann, T.; Englert, U.; Nyulaszi, L.; Baumgartner, T. *Chem.—Eur. J.* **2007**, *13*, 7487.
- (40) Dienes, Y.; Eggenstein, M.; Neumann, T.; Englert, U.; Baumgartner, T. *Dalton Trans.* **2006**, 1424.
- (41) Lampin, J.-P.; Mathey, F. *J. Organomet. Chem.* **1974**, *71*, 239.
- (42) Li, X. C.; Sirringhaus, H.; Garnier, F.; Holmes, A. B.; Moratti, S. C.; Feeder, N.; Clegg, W.; Teat, S. J.; Friend, R. H. *J. Am. Chem. Soc.* **1998**, *120*, 2206.
- (43) Morrison, J. J.; Murray, M. M.; Li, X. C.; Holmes, A. B.; Moratti, S. C.; Friend, R. H.; Sirringhaus, H. *Synth. Met.* **1999**, *102*, 987.
- (44) Sirringhaus, H.; Friend, R. H.; Li, X. C.; Moratti, S. C.; Holmes, A. B.; Feeder, N. *Appl. Phys. Lett.* **1997**, *71*, 3871.
- (45) Kim, O.-K.; Fort, A.; Barzoukas, M.; Blanchard-Desce, M.; Lehn, J.-M. *J. Mater. Chem.* **1999**, *9*, 2227.
- (46) Ventelon, L.; Blanchard-Desce, M.; Moreaux, L.; Mertz, J. *Chem. Commun.* **1999**, 2055.
- (47) Catellani, M.; Boselli, B.; Luzzati, S.; Tripodi, C. *Thin Solid Films* **2002**, *403–404*, 66.
- (48) Frey, J.; Bond, A. D.; Holmes, A. B. *Chem. Commun.* **2002**, 2424.
- (49) Zhang, X.; Matzger, A. J. *Org. Chem.* **2003**, *68*, 9813.
- (50) Casado, J.; Hernández, V.; Kim, O.-K.; Lehn, J.-M.; López Navarrete, J. T.; Delgado Ledesma, S.; Ponce Ortiz, R.; Ruiz Delgado, M. C.; Vida, Y.; Pérez-Inestrosa, E. *Chem.—Eur. J.* **2004**, *10*, 3805.
- (51) Ponce Ortiz, R.; Ruiz Delgado, M. C.; Casado, J.; Hernández, V.; Kim, O.-K.; Woo, H. Y.; López Navarrete, J. T. *J. Am. Chem. Soc.* **2004**, *126*, 13363.
- (52) Sun, Y.; Ma, Y.; Liu, Y.; Lin, Y.; Wang, Z.; Wang, Y.; Di, C.; Xia, K.; Chem, X.; Qui, W.; Zhang, B.; Yu, G.; Hu, W.; Zhu, D. *Adv. Funct. Mater.* **2006**, *16*, 426.
- (53) Hunziker, C.; Zhan, X.; Losio, P. A.; Figi, H.; Kwon, O.-P.; Barlow, S.; Günter, P.; Marder, S. R. *J. Mater. Chem.* **2007**, *17*, 4972.
- (54) Zhan, X.; Tan, Z.; Domercq, B.; An, Z.; Zhang, X.; Barlow, S.; Li, Y.; Zhu, D.; Kippelen, B.; Marder, S. R. *J. Am. Chem. Soc.* **2007**, *129*, 7246.
- (55) Melucci, M.; Favaretto, L.; Bettini, C.; Gazzano, M.; Camaioni, N.; Maccagnani, P.; Ostoj, P.; Monari, M.; Barbarella, G. *Chem.—Eur. J.* **2007**, *13*, 10046.
- (56) Navacchia, M. L.; Melucci, M.; Favaretto, L.; Zanelli, A.; Gazzano, M.; Bongini, A.; Barbarella, G. *Org. Lett.* **2008**, *10*, 3665.
- (57) Zhang, S.; Guo, Y.; Wang, L.; Li, Q.; Zheng, K.; Zhan, X.; Liu, Y.; Liu, R.; Wan, L.-J. *J. Phys. Chem. C* **2009**, *113*, 16232.
- (58) Wu, W.; Liu, Y.; Zhu, D. *Chem. Soc. Rev.*, published on the web. DOI: 10.1039/b813123f.
- (59) Li, J.; Qin, F.; Li, C. M.; Bao, Q.; Chan-Park, M. B.; Zhang, W.; Qin, J.; Ong, B. S. *Chem. Mater.* **2008**, *20*, 2057.
- (60) Santato, C.; Favaretto, L.; Melucci, M.; Zanelli, A.; Gazzano, M.; Monari, M.; Isik, D.; Banville, D.; Bertolazzi, S.; Loranger, S.; Cicoira, F. *J. Mater. Chem.* **2010**, *20*, 669.
- (61) Barbarella, G.; Favaretto, L.; Sotgiu, G.; Antolini, L.; Gigli, G.; Guiseppe, C. R.; Bongini, A. *Chem. Mater.* **2001**, *13*, 4112.
- (62) Gigli, G.; Inanäs, O.; Anni, M.; De Vittorio, M.; Cingolani, R.; Barbarella, G.; Favaretto, L. *Appl. Phys. Lett.* **2001**, *78*, 1493.
- (63) Tedesco, E.; Della Sala, F.; Favaretto, L.; Barbarella, G.; Albesa-Jové, D.; Pisignano, D.; Gigli, G.; Cingolani, R.; Karris, K. D. M. *J. Am. Chem. Soc.* **2003**, *125*, 12277.
- (64) Luzzati, S.; Basso, M.; Catellani, M.; Brabec, C. J.; Gebeyehu, D.; Sariciftci, N. S. *Thin Solid Films* **2002**, *403*.
- (65) Zhang, X. N.; Johnson, J. P.; Kampf, J. W.; Matzger, A. J. *Chem. Mater.* **2006**, *18*, 3470.
- (66) Baumgartner, T. *J. Inorg. Org. Polym. Mater.* **2005**, *15*, 389.
- (67) Rasmussen, S. C.; Ogawa, K.; Rothstein, S. D. In *Handbook of Organic Electronics and Photonics*; Nalwa, H. S., Ed.; American Scientific Publishers: Stevenson Ranch, CA, 2008; Vol. 1.
- (68) Garnier, F.; Hajlaoui, R.; Kassmi, A. E.; Horowitz, G.; Laigre, L.; Porzio, W.; Armanini, M.; Provasoli, F. *Chem. Mater.* **1998**, *10*, 3334.
- (69) Horowitz, G.; Hajlaoui, R.; Fichou, D.; El Kassmi, A. *J. Appl. Phys.* **1999**, *85*, 3202.
- (70) Hajlaoui, R.; Horowitz, G.; Garnier, F.; Arce-Bouchet, A.; Laigre, L.; El Kassmi, A.; Demanze, F.; Kouki, F. *Adv. Mater.* **1997**, *9*, 389.
- (71) Letizia, J. A.; Facchetti, A.; Stern, C. L.; Ratner, M. A.; Marks, T. J. *J. Am. Chem. Soc.* **2005**, *127*, 12476.
- (72) Although the alkyl groups used in the present study vary from compound to compound, they are all of sufficient length that the variation in inductive electron donation between them is anticipated to be negligible.
- (73) Anni, M.; Della Sala, F.; Raganato, M. F.; Fabiano, E.; Lattante, S.; Cingolani, R.; Gigli, G.; Barbarella, G.; Favaretto, L.; Görling, A. *J. Phys. Chem. B* **2005**, *109*, 6004.
- (74) Sánchez-Carrera, R. S.; Odom, S. A.; Kinnibrugh, T. L.; Sajoto, T.; Kim, E.-G.; Timofeeva, T. V.; Barlow, S.; Coropceanu, V.; Marder, S. R.; Brédas, J. L. *J. Phys. Chem. B* **2010**, *114*, 749.
- (75) Kwon, O.; Barlow, S.; Odom, S. A.; Beverina, L.; Thompson, N. J.; Zojer, E.; Brédas, J.-L.; Marder, S. R. *J. Phys. Chem. A* **2005**, *109*, 9346.
- (76) Fujitsuka, M.; Sato, T.; Sezaki, F.; Tanaka, K.; Watanabe, A.; Ito, O. *J. Chem. Soc., Faraday Trans.* **1998**, *94*, 3331.
- (77) Odom, S. A.; Lancaster, K.; Beverina, L.; Lefler, K. M.; Thompson, N. J.; Coropceanu, V.; Brédas, J.-L.; Marder, S. R.; Barlow, S. *Chem.—Eur. J.* **2007**, *13*, 9637.
- (78) Ehrenson, S.; Brownlee, R. T. C.; Taft, R. W. *Prog. Phys. Org. Chem.* **1973**, *10*, 1.
- (79) Hansch, C.; Leo, A.; Taft, R. W. *Chem. Rev.* **1991**, *91*, 165.
- (80) Taft, R. W.; Lewis, I. C. *J. Am. Chem. Soc.* **1958**, *80*, 2436.
- (81) The σ_1 values used for the X groups of compounds **a–l** were as follows: 0.00, −0.05, −0.07, 0.27, 0.10, 0.12, 0.12, 0.05, 0.40, 0.25, 0.50, and 0.59, respectively. Where possible, the values used were those for the corresponding XMe substituent and were taken from: Lowry, T. H.; Schueller Richardson, K. *Mechanism and Theory in Organic Chemistry*, 3rd ed.; Harper Collins: New York, 1987. March, J. *Advanced Organic Chemistry*; Wiley: New York, 1985. Or ref 79. For X = PPh and P(O)Ph (**h** and **i**, respectively), values for XMe = PMe₂ and P(O)Me₂ were used, while for the two X = NAr groups (**f** and **g**), values for NPh₂ were used. Approximations of this type, coupled with the fact that, for some X groups, alternative estimates of σ_1 are available (see, for example, the tables in ref 79), mean that any correlations of physical data with these parameters are inevitably going to be approximate.
- (82) Pasini, M.; Destri, S.; Botta, C.; Porzio, W. *Tetrahedron* **1999**, *55*, 14985.
- (83) de Jong, F.; Janssen, M. J. *Chem. Soc., Perkin II* **1972**, 572.
- (84) Koster, P. B.; Janssen, M. J.; Lucken, E. A. C. *J. Chem. Soc., Perkin II* **1974**, 803.
- (85) The fluorescence maximum of **1a** is very similar to that previously reported for the same compound in THF (ref 85). The fluorescence signals exhibited by **1e**, **1f**, and **1j** were all very weak, consistent with previous reports of low fluorescence quantum yields for the analogous species without 2,6-alkylation (refs 24 and 76); accordingly, wide emission slit settings (3 nm) and complications arising from adequately correcting for solvent Raman signals lead to less precisely determined maxima than for **1a** and compounds of type **2**.
- (86) Facchetti, A.; Yoon, M.-H.; Stern, C. L.; Hutchison, G. R.; Ratner, M. A.; Marks, T. J. *J. Am. Chem. Soc.* **2004**, *126*, 13480.
- (87) San Miguel, L.; Porter, W. W.; Matzger, A. J. *Org. Lett.* **2007**, *9*, 1005.
- (88) Amer, A.; Burkhardt, A.; Nkansah, A.; Shabana, R.; Galal, A.; Mark, H. B.; Zimmer, H. *Phosphorus, Sulfur Silicon Relat. Elem.* **1989**, *42*, 63.
- (89) Pasini, M.; Destri, S.; Botta, C.; Porzio, W. *Synth. Met.* **2000**, *113*, 129.
- (90) DiCésare, N.; Belletête, M.; Raymond, F.; Leclerc, M.; Durocher, G. *J. Phys. Chem. A* **1997**, *101*, 776.
- (91) Connelly, N. G.; Geiger, W. E. *Chem. Rev.* **1996**, *96*, 877.
- (92) Barlow, S.; Risko, C.; Chung, S.-J.; Tucker, N. M.; Coropceanu, V.; Jones, S. C.; Levi, Z.; Brédas, J. L.; Marder, S. R. *J. Am. Chem. Soc.* **2005**, *127*, 16900.
- (93) The calculations indicate that many configurations contribute to these higher-lying states, with no single configuration dominating the description.
- (94) Fujitsuka, M.; Sato, T.; Shimidzu, T.; Watanabe, A. *J. Phys. Chem. A* **1997**, *101*, 1056.
- (95) Fichou, D.; Horowitz, G.; Xu, B.; Garnier, F. *Synth. Met.* **1990**, *39*, 243.
- (96) Yu, Y.; Gunic, E.; Zinger, B.; Miller, L. L. *J. Am. Chem. Soc.* **1996**, *118*, 1013.

(97) Guay, J.; Kasai, P.; Diaz, A.; Wu, R.; Tour, J. M.; Dao, L. H. *Chem. Mater.* **1992**, *4*, 1097.

(98) The radical cations of some oligothiophenes are known to form diamagnetic π -dimers: Audebert, P.; Hapiot, P.; Pernaut, J.-M.; Garcia, P. *J. Electroanal. Chem.* **1993**, *361*, 283. Graf, D. D.; Duan, R. G.; Campbell, J. P.; Miller, L. L.; Mann, K. R. *J. Am. Chem. Soc.* **1997**, *119*, 5888. The paramagnetism and the vis-NIR spectra suggest that this type of dimerization is not significant for the present species in dichloromethane. However, additional weak features present at low energy in the spectra of some of these cations (see the spectra shown in the Supporting Information for $2b^{+}$, $2i^{+}$, and $2k^{+}$) may possibly be due to the presence of low concentrations of dimeric species. In the case of $2b^{+}$, we found that these

additional features were lost when the oxidation reaction was repeated with the same oxidant concentration but a decreased excess of $2b$ (see Figure S10, Supporting Information); accordingly, it appears that these features are due to species arising from interactions between the radical cations and the corresponding neutral species, such as monocationic π dimers.

(99) Duling, D. R. *J. Magn. Reson. Ser. B* **1994**, *104*, 105.

(100) <http://www.niehs.nih.gov/research/resources/software/tools/index.cfm>.

(101) Kirste, B.; Tian, P.; Kossmehl, G.; Engelmann, G.; Jugelt, W. *Magn. Reson. Chem.* **1995**, *33*, 70.

JP100774R